

Particle and surfactant interactions effected polar and dispersive components of interfacial energy in nanocolloids

A. R. Harikrishnan, , Sarit K. Das, , Prabhat K. Agnihotri, and , and Purbarun Dhar

Citation: *Journal of Applied Physics* **122**, 054301 (2017); doi: 10.1063/1.4997123

View online: <http://dx.doi.org/10.1063/1.4997123>

View Table of Contents: <http://aip.scitation.org/toc/jap/122/5>

Published by the *American Institute of Physics*

Articles you may be interested in

[Predicting thermal history a-priori for magnetic nanoparticle hyperthermia of internal carcinoma](#)
Journal of Applied Physics **122**, 054902 (2017); 10.1063/1.4997471

[Importance of frequency dependent magnetoresistance measurements in analysing the intrinsicity of magnetodielectric effect: A case study](#)
Journal of Applied Physics **122**, 054103 (2017); 10.1063/1.4997473

[Barium hydroxide hole blocking layer for front- and back-organic/crystalline Si heterojunction solar cells](#)
Journal of Applied Physics **122**, 055101 (2017); 10.1063/1.4985812

[Transition metal partially supported graphene: Magnetism and oscillatory electrostatic potentials](#)
Journal of Applied Physics **122**, 055303 (2017); 10.1063/1.4997467

[Measuring the flexoelectric coefficient of bulk barium titanate from a shock wave experiment](#)
Journal of Applied Physics **122**, 055106 (2017); 10.1063/1.4997475

[Effect of shear stress in ferroelectric solid solutions with coexisting phases](#)
Journal of Applied Physics **122**, 054102 (2017); 10.1063/1.4994171



AIP | Journal of Applied Physics

Save your money for your research.
It's now **FREE** to publish with us -
no page, color or publication charges apply.

Publish your research in the
Journal of Applied Physics
to claim your place in applied
physics history.

Particle and surfactant interactions effected polar and dispersive components of interfacial energy in nanocolloids

A. R. Harikrishnan,¹ Sarit K. Das,^{1,a)} Prabhat K. Agnihotri,^{2,a)} and Purbarun Dhar^{2,a)}

¹Department of Mechanical Engineering, Indian Institute of Technology Madras, Chennai 600036, India

²Department of Mechanical Engineering, Indian Institute of Technology Ropar, Rupnagar 140001, India

(Received 18 May 2017; accepted 21 July 2017; published online 1 August 2017)

We segregate and report experimentally for the first time the polar and dispersive interfacial energy components of complex nanocolloidal dispersions. In the present study, we introduce a novel inverse protocol for the classical Owens Wendt method to determine the constitutive polar and dispersive elements of surface tension in such multicomponent fluidic systems. The effect of nanoparticles alone and aqueous surfactants alone are studied independently to understand the role of the concentration of the dispersed phase in modulating the constitutive elements of surface energy in fluids. Surfactants are capable of altering the polar component, and the combined particle and surfactant nanodispersions are shown to be effective in modulating the polar and dispersive components of surface tension depending on the relative particle and surfactant concentrations as well as the morphological and electrostatic nature of the dispersed phases. We observe that the combined surfactant and particle colloid exhibits a similar behavior to that of the particle only case; however, the amount of modulation of the polar and dispersive constituents is found to be different from the particle alone case which brings to the forefront the mechanisms through which surfactants modulate interfacial energies in complex fluids. Accordingly, we are able to show that the observations can be merged into a form of quasi-universal trend in the trends of polar and dispersive components in spite of the non-universal character in the wetting behavior of the fluids. We analyze the different factors affecting the polar and dispersive interactions in such complex colloids, and the physics behind such complex interactions has been explained by appealing to the classical dispersion theories by London, Debye, and Keesom as well as by Derjaguin-Landau-Verwey-Overbeek theory. The findings shed light on the nature of wetting behavior of such complex fluids and help in predicting the wettability and the degree of interfacial interaction with a substrate in such multicomponent nanocolloidal systems. *Published by AIP Publishing.*

[<http://dx.doi.org/10.1063/1.4997123>]

I. INTRODUCTION

Interfacial interactions in the case of nanocolloids are a complex phenomenon due to the large number of interacting forces at the molecular and nanoscale levels. Recent research has been focusing on the interfacial aspects of nanocolloidal dispersions such as interfacial tension,^{1,2} wettability,^{3,4} and evaporation characteristics⁵⁻⁸ due to their unique properties which are capable of tuning and improving the performance in various fields of engineering. The degree of wettability, usually characterized by the magnitude of the equilibrium contact angle, depends on the interfacial interactions at the molecular scale. These interfacial interactions are governed by the gross interfacial energies of all the interfaces involved, often denoted as the surface energy. There are different and well established methods such as the method of Girifalco and Good,⁹ Focks method,^{10,11} Owens Wendt method,^{12,13} Van Oss Chaudhury method,¹⁴ etc., to characterize the surface energy of a surface. The Owens Wendt method, one of the most widely used and recognized method, uses contact angle data to measure the interfacial energy in

terms of polar and dispersive interactions with the test or calibration fluids possessing known polar and dispersive components of surface tension. The polar and dispersive components of surface tension of common fluids are well characterized and reported¹⁵⁻¹⁷ in the literature. The knowledge of these elements of surface tension finds application in various engineering fields such as for assessing the wettability of a substrate, in the coatings and paint industry for deciding the quality and suitability of the coating, in printing technology, targeted drug delivery,^{18,19} etc.

The present study reports for the first time the role of nanoparticles in modulating the dispersive and polar elements of interfacial energy and the role of surfactants in the process, and this is reported for the first time to the best of the authors' knowledge. The present study employs an inverse Owens Wendt method in order to calculate the polar and dispersive interactions in multicomponent nanocolloidal dispersions. The Owens Wendt method is applied to the surfaces of known polar and dispersive interactions to identify the polar and dispersive interactions in complex nanocolloids. Also, an in-depth analysis has been presented on the nature of variations of such interactions in aqueous surfactant solutions alone, nanoparticles only based colloid case and in the case of combined surfactant infused nanocolloidal

^{a)} Authors to whom correspondence should be addressed: skdas@iitrpr.ac.in; prabhat@iitrpr.ac.in; and purbarun@iitrpr.ac.in, pdhar1990@gmail.com, Telephone: +91-1881-24-2173.

systems with respect to the concentration of the dispersed phase. The dynamic development and steadily increasing scope of nanofluids in various domains of engineering and the biological domain stimulate a better reorganization and a deeper understanding of interaction properties among the constituents of such complex fluids for improving functionality and applicability.

II. EXPERIMENTAL METHODOLOGY

Experiments for the present work have been planned in such a manner that the effect of surfactant molecules alone, the effect of particles alone and the combined effect of surfactant and particles in modulating the constituent components of surface tension can be extracted. Five types of nanoparticles, viz., CuO (~ 30 nm, NanoArc, Alfa Aesar, India), Al_2O_3 (~ 45 nm, Sigma Aldrich, USA), Bi_2O_3 (~ 20 nm, Alfa Aesar, India), SiO_2 (~ 45 nm, Sigma Aldrich, USA) and multiwalled carbon nanotubes (MWCNTs) (20–40 nm external diameter and aspect ratio ~ 100 , Sisco Research Lab, India) and two types of stabilizing agents, viz., sodium dodecyl sulphate (SDS) (anionic, 99% pure, Sisco Research Labs, India), cetyl trimethyl ammonium bromide (CTAB) (cationic, 99.5% pure, Sisco Research Labs, India) have been considered in the present study. Figure 1 illustrates the morphological characteristics of different nanoparticles considered in the present study as visualized during High Resolution Scanning Electron Microscopy (HRSEM) and TEM characterization. Figure 1(a) shows the high resolution scanning electron microscope (HRSEM) image of Al_2O_3 with spherical morphology and Fig. 1(b) illustrates the flake-like morphology of Bi_2O_3 with a flake thickness of around ~ 16 nm and an average flake face length of around ~ 300 nm. Figure 1(c) shows the hexagonal pillar structure of ZnO with an average dimension of 50 nm–90 nm as the face width of the pillar. Figure 1(d) illustrates the HRSEM characterization of MWCNTs, Fig. 1(e) shows the characterization of SiO_2 and Fig. 1(f) illustrates the HRSEM

characterization of CuO (30 nm) nanoparticles indicating an oblate spherical morphology.

The weighted amount of nanoparticles is dispersed in accurately measured volume of deionized (DI) water (Millipore, electrical conductivity $1\text{--}3\ \mu\text{S}/\text{cm}$) and sonicated (Oscar Ultrasonics, India) for the requisite amount of time to ensure phase stability. Four commonly used engineering surfaces with a range of wettability have been selected for the present study, viz., glass slides (the slides are rendered uniformly hydrophilic in nature by exposing to argon plasma treatment), single crystal silicon wafer (200 nm SiO_2 layer thick wafer, $\langle 100 \rangle$ crystal orientation, hydrophilic), copper (Cu 101 oxygen-free copper, partially hydrophobic, average surface roughness $R_a \sim 0.255 \pm 0.085\ \mu\text{m}$) and aluminium (Al 6061 grade, near hydrophobic in nature, $R_a \sim 1.091 \pm 0.095\ \mu\text{m}$). The surface roughnesses have been characterized in orthogonal directions at different locations on the substrate employing a roughness profile measurement device (Handysurf, USA). In order to segregate and understand the individual and combined effects of surfactants and particles, first, a set of experiments of contact angle measurements have been conducted on the substrates with a base fluid (DI water), which form the reference data. The equilibrium contact angles have been measured by employing sessile drop technique using a contact angle goniometer (First Ten Angstroms, USA) by fitting the curve to the captured video frame.

The second set of experimental run was conducted with nanofluids prepared by dispersing the particle alone without the aid of surfactants. Before the next set of experiments with combined particle and surfactants, a set of experimental run was conducted with aqueous surfactant solution only. This has generated a set of contact angle data on all the substrates considered in the present study at different concentrations of the dispersed phases. The substrates were pre-cleaned by dipping in acetone solution (isopropanol for the Si surfaces) and then in DI water and then dried in an oven before each set of experiments. The particle concentration has been varied from 0.1 wt. % up to 2.5 wt. % in the case of

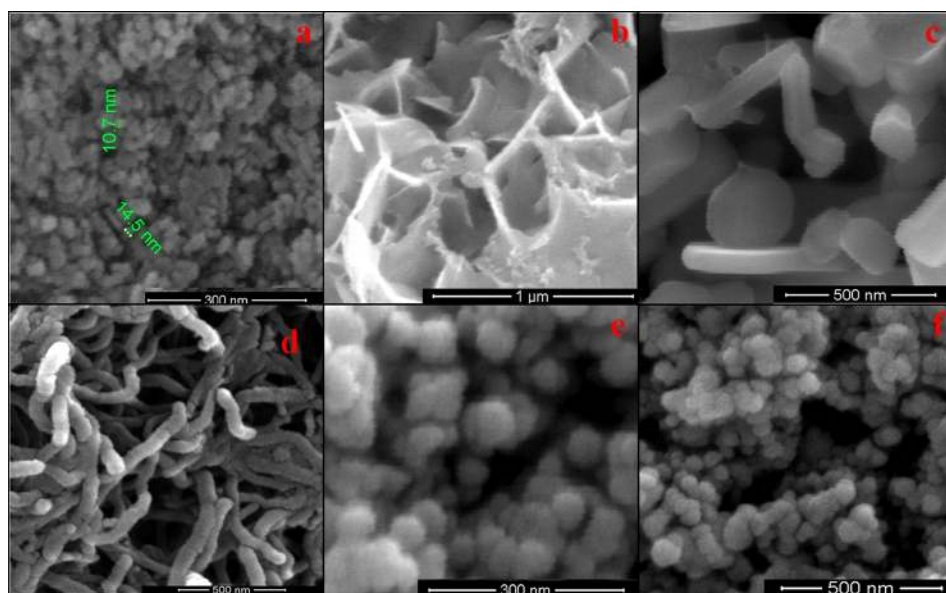


FIG. 1. (a) HRSEM image of Al_2O_3 with a spherical morphology of ~ 13 nm, (b) Bi_2O_3 nanoparticles showing the flake morphology with a flake width of ~ 20 nm, (c) ZnO nanostructures with a hexagonal rod structure with an average dimension of ~ 80 nm, (d) HRSEM characterization of MWCNTs, (e) HRSEM characterization of SiO_2 , and (f) HRSEM characterization of CuO (30 nm) nanoparticles.

TABLE I. Properties of the test fluids employed as references.

| SI. No | Test fluid | Total surface tension (mN/m) | Dispersive component (mN/m) | Polar component (mN/m) | Reference |
|--------|------------|------------------------------|-----------------------------|------------------------|-----------|
| 1. | Water | 72.8 | 22.6 | 50.2 | 12, 15–17 |
| 2. | DMSO | 44 | 36 | 8 | 12 |

metal oxide nanoparticles and from 0.01 wt. % to 0.25 wt. % in the case of MWCNTs in order to understand the particle concentration effect, and the surfactant concentration was varied from 0.25 Critical Micelle Concentration (CMC) up to 1 CMC in order to capture the effect of a surfactant for a given particle concentration. The CMCs for the above selected surfactants are fixed as per reported literature.¹ All the experiments were carried out at $30 \pm 2^\circ\text{C}$ and under relative humidity conditions of $50 \pm 5\%$. In order to characterize the surfaces and measure the surface energy of the test surfaces, two test fluids are considered, viz., DI water (*in situ* purified, Millipore, $\sim 3 \mu\text{S}/\text{cm}$) and DMSO (Dimethyl sulfoxide) (99% pure, Avra Synthesis, India), and their properties are listed in Table I. The Oven Wendt method has been employed in determining the surface free energy of the substrates considered in the present study by making use of the contact angle measurement data with the test fluids. The thus calculated surface energies along with the experimental results of contact angle measurements are used in the Owens Wendt equation of state [Eq. (2)] to extract the dispersive and polar components of surface tension.

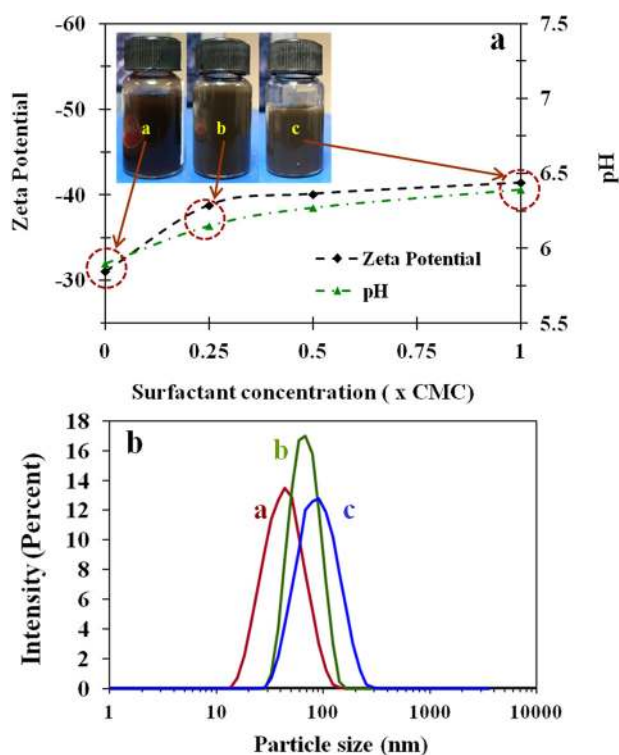


FIG. 2. (a) Zeta potential and pH variation with surfactant concentration for CuO based nanofluids. The fluids represented in the inset are: a-CuO nanofluid, b-CuO and 0.25 CMC SDS, c-CuO and 1.0 CMC SDS. (b) Particle size analysis intensity versus particle size curve for the above three fluids.

Figure 2(a) illustrates CuO nanofluids prepared without surfactant addition and also with 0.25 CMC and 1.0 CMC concentrations of SDS surfactant. Figure 2(a) illustrates the zeta potential and pH variation of the three types of nanofluids, viz., a-CuO nanofluid, b-CuO with 0.25 CMC SDS, and c-CuO and 1.0 CMC SDS. With the increase in the surfactant concentration for a given particle concentration, the zeta potential and the magnitude of the pH increase. The numerical value of the zeta potential lies outside the zone between -30 and 30 mV, which indicates a good phase stability of the nanocolloids. Figure 2(b) illustrates the Dynamic Light Scattering (DLS) (Malvern Instruments) analysis of the above three fluids. A shift in the maximum intensity peak towards the right (higher effective particle diameter or hydrodynamic diameter) can be observed with the increase in the surfactant concentration. As the concentration of the surfactant in the nanocolloid increases, the effective hydrodynamic diameter [particle diameter plus twice the Electrical Double Layer (EDL) thickness] of the particle increases due to the increase in the thickness of the EDL (which may be obtained from the associated Debye length). The observation is reinforced from the results of zeta potential measurements with increasing surfactant concentration as illustrated in Fig. 2(a). The trend is found to be similar in the case of other nanocolloidal suspensions also. The observable increase in the zeta potential with surfactant concentration can be attributed to the enhanced Debye layer thickness as well as enhanced charged species within the Stern-Helmholtz layer, thereby presenting evidence of the surfactant chains capping the particle surface.

III. THEORY AND METHODOLOGY

The classical Young's equation relates the surface free energy (SFE) of the substrate and the fluid with the static contact angle for the fluid-substrate pair. But, obtaining the magnitude of the interfacial tension at the solid-liquid interface poses a challenge and hence numerous research works are attributed to establishing the so-called equation of state, which is based on the primary assumption that the interfacial free energy at the liquid-solid interface is a function of the participating fluid, and solid free energies and can be expressed in a closed function form as

$$F(\gamma_l, \gamma_s, \gamma_{sl}) = 0, \quad (1)$$

where γ_l is the liquid surface tension, γ_s is the solid surface tension or surface energy, and γ_{sl} is the solid-liquid interfacial tension. Numerous works have been directed in this regard to develop a relation between the properties of interacting solid and fluid media and the interfacial free energy at the interface of both.^{10–14,20} The pioneering work by Fowkes^{10,11} considered the surface free energy (SFE) of the solid as a summation of the independent components due to different interactions such as dispersion, polar, hydrogen bonding and other interactions which pose significance in microscale fluidics. According to Fowkes, the dispersion component of the SFE is connected with the London interactions, arising from the electron dipole fluctuations. These

interactions occur commonly in matter and result from the attraction between adjacent atoms and molecules. The London forces depend on the kind of mutually attracting elements of the involved matter and are independent of other types of interactions. The remaining van der Waals form of interactions, i.e., the Keesom and Debye interactions, have been considered by Fowkes as a part of inducing interactions. Owens Wendt^{12,13} proposed the following relation [Eq. (2)] based on Fowkes proposal for partitioning the surface energy into components:

$$\gamma_{sl} = \gamma_s + \gamma_l - 2(\gamma_s^d \gamma_l^d)^{0.5} - 2(\gamma_s^p \gamma_l^p)^{0.5}, \quad (2)$$

where γ_{sl} is the solid liquid interfacial tension, γ_s is the solid surface energy, γ_l is the liquid surface tension, γ_s^d and γ_s^p represent the dispersive and polar components of the solid surface energy and similarly γ_l^d and γ_l^p represent the dispersive and polar components of the liquid counterpart. The subscripts “s” and “l” stand for the solid and the liquid, respectively. Combining the above equation with the basic Young equation of state

$$\gamma_{sl} = \gamma_s - \gamma_l \cos\theta, \quad (3)$$

a linear equation of the form $Y = mX + C$ can be arrived at, which is expressed as

$$Y = \frac{\gamma_l(1 + \cos\theta)}{2\sqrt{\gamma_l^d}} = \underbrace{\sqrt{\frac{\gamma_l^p}{\gamma_l^d}}}_B \sqrt{\gamma_s^p} + \underbrace{\sqrt{\gamma_s^d}}_A, \quad (4)$$

where the Y and X components in the linear form are denoted as A and B, respectively, as shown above. The methodology outlined by the Owens Wendt protocol requires contact angle data for a minimum of two test fluids (whose polar and dispersive components of surface tension are known). Hence, from the contact angle data for at least two test fluids whose polar and dispersive components of surface tension as well as the total surface tension are known, a linear fit can be made as illustrated in Fig. 3(a). The square of the slope corresponds to the polar components of the solid, and the square of the intercept will give the dispersive component of the solid. Figure 3 shows the Owens Wendt plot according to Eq. (4) for the test fluids for all the four substrates in the present study. The polar and dispersive components of the surfaces considered in the present study are illustrated in Figs. 3(b) and 3(c). In aluminium and copper substrates, the dispersive interaction dominates over polar interactions, whereas in the case of glass and silicon wafer, the polar nature of surface free energy is the major contributor to total surface energy.

The surface regression/interfacial region as coined by Fowkes¹⁰ is responsible for the surface tensional characteristics, which in itself comprises the surface or the interfacial monolayer and the adjacent bulk liquid. Molecules in the surface region of the liquid are subject to attractive forces from adjacent molecules which result in a net attraction to the bulk phase in the direction normal to the surface. The

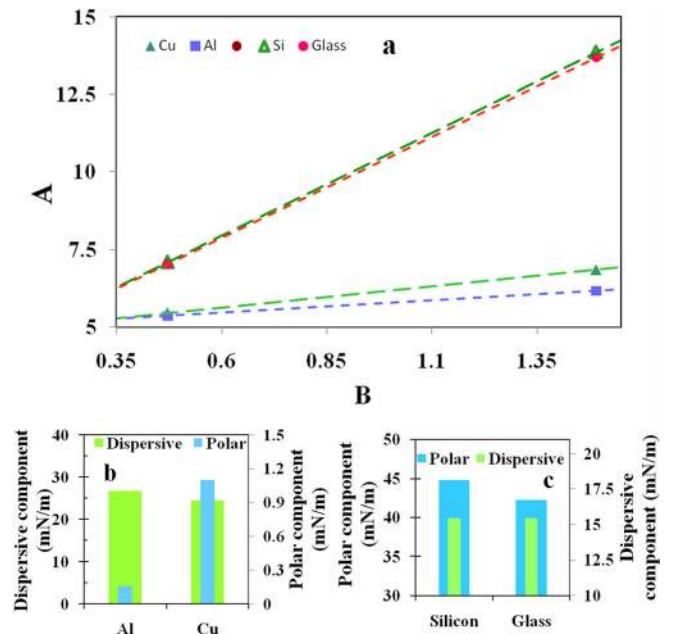


FIG. 3. (a) Linear fit for extracting polar and dispersive components; (b) polar and dispersive components for aluminium and copper substrates (c) and for silicon and glass.

attraction tends to reduce the number of molecules in the interfacial region which results in an increase in the intermolecular distance. Drawing an analogy with respect to a spring system will bring out the physics behind the existence of surface energy. There are different forms of intermolecular forces which are jointly manifested in the form of surface tension force. A major component among these interactions which is present in all the substances is the London dispersion force that arises from the interaction of fluctuating electronic dipoles with induced dipoles in neighboring atoms or molecules. These forces are functions of electrical properties of the volumetric elements involved in the concerned material and also the distance between them. However, these are independent of temperature, and are in itself a fundamental form of interaction. DLVO (Derjaguin-Landau-Verwey-Overbeek) theory^{21,22} underlines and dictates the basic interaction modes in such colloidal dispersions and takes into consideration the fundamental interactions of the van der Waals attractive force and the electrostatic repulsive interaction. The summation of these two basic interactions will give the total DLVO forces which essentially is a pin-pointing entity towards colloidal phase stability and characteristics.

The later advancement in the theory has incorporated additional interactive forces. The coupled dipole method (CDM), a method introduced by Kwaadgras *et al.*,²³ considers each atom in a cluster as a Lorentz particle in which the electron is bound to the nucleus by a harmonic force. The atoms have no permanent electric dipole moment, but their dipole moments are induced by the local imposed electric field. This can be used to compute the van der Waals interactions between the atoms, and its inherent many-body nature made it more accurate than continuum theories based on pairwise summations of atomic van der Waals interactions, as employed in, e.g., the Hamaker-de Boer approach²⁴ that

underlies the treatment of dispersion forces in DLVO-theory. In this article, the solvent effects are not considered explicitly. Since an electric dipole will produce a non-zero electric field in its surroundings, two of these Lorentz atoms will interact, mediated by the electric field. The other contribution to the van der Waals interaction, as outlined earlier, comprises the Keesom interaction which is an orientation governed interaction force and the other component is the Debye interaction which is an induction interaction.²⁵ Polar interactions comprise Coulomb interactions between permanent dipoles and between permanent and induced dipoles (e.g., hydrogen bonds). The formation of an EDL and the permanent dipole interaction because of the EDL, acid base interactions, hydrogen bonding, etc., together contribute towards the polar component of surface tension.

In the present study, the same method is being used to determine the polar and dispersive components of nanocolloidal suspensions, i.e., the constituents of the complex liquid-gas interfacial tension. Contact angle measurements of the nanocolloidal suspensions are done on all the substrates considered in the present study at different concentrations of particles and surfactants. With the surfaces of known polar and dispersive components and contact angle information from the experiments and using Eq. (5), a modified version obtained by rearranging the equation outlined by Owens Wendt, the polar and dispersive components of colloidal solutions are arrived at from the slope and the intercept of the linear fit made for the four data points with the data on four substrates

$$\frac{\gamma_l(1 + \cos\theta)}{2\sqrt{\gamma_s^d}} = \sqrt{\frac{\gamma_s^p}{\gamma_s^d}}\sqrt{\gamma_l^p} + \sqrt{\gamma_l^d}. \quad (5)$$

A detailed algorithm of the methods followed for deriving the polar and dispersive constituents in colloidal solution is described in [supplementary material](#).

IV. RESULTS AND DISCUSSION

The polar and dispersive constituents of surface tension in the case of aqueous surfactant solutions at different concentrations of surfactants are illustrated in Fig. 4(a). The nature of variation of interfacial energy components is found to be independent of the nature of the surfactant (anionic or cationic), and observed to be similar for all the surfactants considered in the present study. It is an established fact that the addition of surfactants is capable of lowering the surface tension of the base fluid²⁶ because of the interfacial adsorption of the surfactants onto the interfaces. When an aqueous surfactant solution drop is placed on the substrate, the surfactant molecules will adsorb at the liquid-solid interface and the liquid-air interface. The rate of adsorption onto these interfaces depends on the nature of the surfactant and the surfaces. These will alter the liquid-solid interfacial energy and the liquid-air interfacial energy. This will be reflected in the form of a macroscopic contact angle of the aqueous solution on the given substrate.^{27,28} The total surface tension of the aqueous surfactant solution decreases with surfactant concentration till the CMC because of the interfacial adsorption of surfactants at the liquid-air interface.¹ Therefore, the ratio

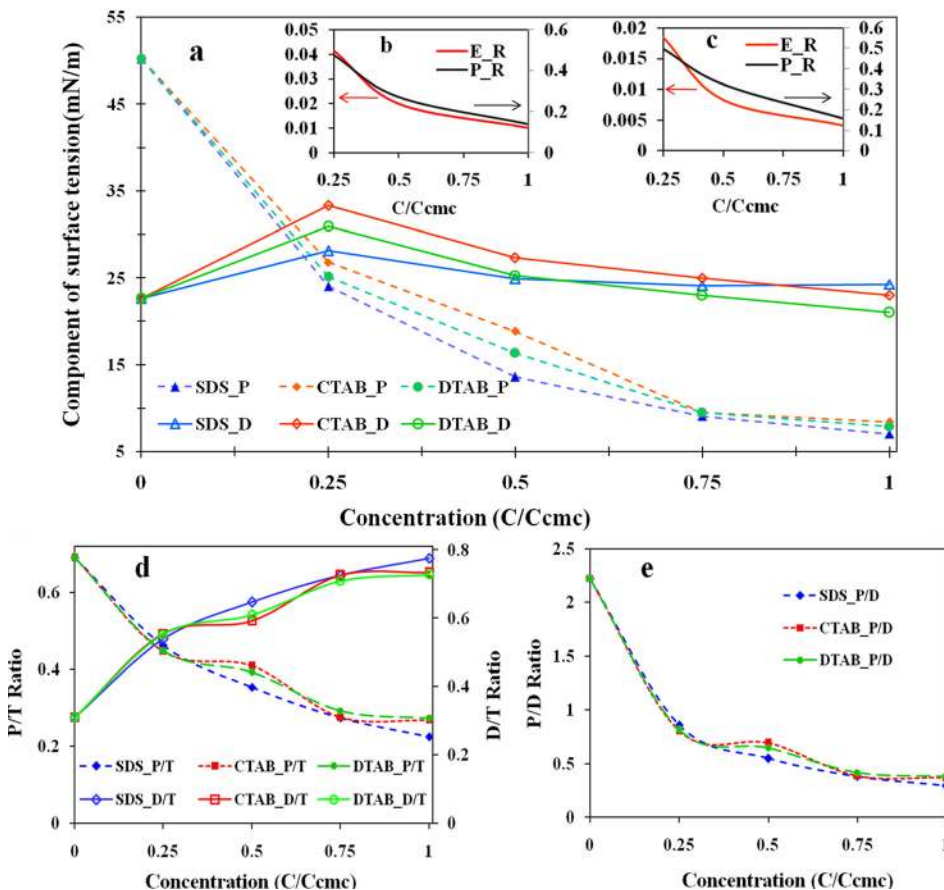


FIG. 4. (a) Variation of polar and dispersive components of surface tension for various aqueous surfactant solutions with surfactant concentration. The electrical conductivity ratio (E_R) and the polar component ratio (P_R) of aqueous surfactant solution to water for (b) SDS and (c) CTAB. (d) Variation of polar and dispersive components of surface tension to total surface tension of various aqueous surfactants at different concentrations and (e) the ratio of components of surface tension to surfactant concentration.

of the polar or dispersive component of surface tension to that of the total surface tension represents the actual scenario with a better enlightenment to the actual physics of the problem. Figure 4(b) illustrates the ratio of polar and dispersive components of surface tension to the total surface tension of all the surfactants in the present study. The surfactant concentration corresponding to zero represents the base fluid, i.e., DI water. The concentration of the surfactant is varied from one fourth of CMC to the CMC, as the present study is not interested in the postmicellar characteristics. Apparently, though it can be observed that the numerical value of the polar and dispersive components of three surfactants are slightly different in magnitude [as illustrated in Fig. 4(a)], the ratio of the polar or dispersive component of surface tension to that of the total surface tension (P/T or D/T ratio) for all the surfactants is coinciding, as illustrated in Fig. 4(d). The ratio of the polar component of surface tension to that of the total surface tension (P/T ratio) decreases with an increase in surfactant concentration, whereas the normalized ratio of the dispersive component with the total surface tension (D/T ratio) increases with surfactant concentration. Both the normalized curves reach a plateau towards the CMC. The normalized components of surface tension are found to be independent of the nature and properties of surfactants as they take into account the interfacial adsorption and hence the interactions at the interfaces.

The ratio of polar to dispersive components of the surface tension is illustrated in Fig. 4(e). The polar to dispersive ratio (P/D ratio) magnitude greater than unity indicates a predominant contribution of the polar component to the total surface tension of the solution. Interestingly, the ratio of the polar to dispersive components of surface energy is similar for all the surfactants under consideration even though the wetting angle made by each surfactant on different substrates and the surface tension of different surfactants at different concentrations of surfactants are different from each other. There is an observable dominance of polar nature up to one fourth of the micellar concentration, and thereafter the dispersive interaction is the dominant part of total surface tension. The strong tiled relation and the nature of variation with respect to the surfactant concentration existing between the electrical conductivity ratio (E_R) (ratio of electrical conductivity of the surfactant to that of the electrical conductivity of water) and the ratio of the polar component of surface tension of aqueous surfactant to that of water (P_R) further strengthen the theoretical root of variation of the polar component as illustrated in Figs. 4(b) and 4(c). The ratio of electrical conductivities and the ratio of polar components are directly related and vary in a similar manner. The values of electrical conductivity for different aqueous surfactant solutions are directly taken from the observations of Herrington *et al.*²⁹ The ionic conductivity in these aqueous surfactant solutions is directly related to the degree of ionisation produced due to the dispersion of surfactants, and the degree of ionic interactions in the solutions adds up to the polar nature of the solution and is directly related to the amount of surfactant molecules available in the bulk of the solution. Hence, both the phenomena are directly linked with each other. Both the non-dimensional ratios vary in a similar

fashion and both decrease with the increase in surfactant concentration. As the surfactant concentration increases, the van der Waals interaction between the surfactant chains increases which results in building the total dispersive interactions in the solution. Even though the magnitude of the dispersive component seems to not change much, the ratio of the dispersive part to the total surface tension increases. This is due to the fact that the total surface tension of the aqueous surfactant also decreases with an increase in the surfactant concentration.

At the same moment, the inclusion of surfactant molecules and their interfacial adsorption will disrupt the strong hydrogen bonding in water which results in the reduction of the polar nature of water. As the surfactants are dispersed in water, the ionic head of the surfactant molecules will form an ionic interaction with the polar water molecule, and the net resultant polarity of the solution decreases. The polar end will be attracted to either the negatively charged oxygen or the positively charged hydrogen in water depending on the nature of the surfactant. The covalent tails will separate from the H₂O molecules and migrate to the surface. Water molecules will be attracted to the polar end of the surfactant, while the covalent tails will not interact with water and separate. The lower attraction of covalent tails to each other will make it easier to separate the molecules. As the surfactant concentration increases, the polar component keeps on decreasing up to the micellar concentration, as can be observed from Figs. 4(a) and 4(d). Once the micellization has happened, the ionic heads are no longer active in bringing down the polarity of the solution. Also, the dispersive component of surface tension curve also saturates near the micellar concentration. As the present study is interested in only the pre-micellar characteristics of the aqueous surfactant solution, the study has not been extended to the post-micellar region.

The nature of variation of the ratio of polar or dispersive component of surface tension to the total surface tension in the case of colloidal dispersion of nanoparticles alone is illustrated in Fig. 5(a). The polar to total surface tension decreases and attains a plateau with the particle concentration, whereas the dispersive to total surface tension ratio increases and then saturates with the particle concentration. The amount and the rate of increment or decrement in surface tension ratio depend on the nature of particles and are different for different particles unlike as observed in the case of different aqueous surfactants. It is also noteworthy that from a previous report by the present authors¹ one can conclude that the total surface tension of such complex fluids increases with particle concentration. It has been elucidated from the previous study that the establishment of total equilibrium is considered to be the reason for the effective increment in surface tension of nanocolloidal solutions only as the adsorbed particles are subjected to many interaction forces. SiO₂ is shown to have a maximum increase in the dispersive component to the total surface tension and the hence a minimum value of polar to total surface tension ratio. Except for the anomalous behavior of SiO₂ nanoparticles, almost all the other nanoparticles attained the saturation limit with respect to a change in the particle concentration at a

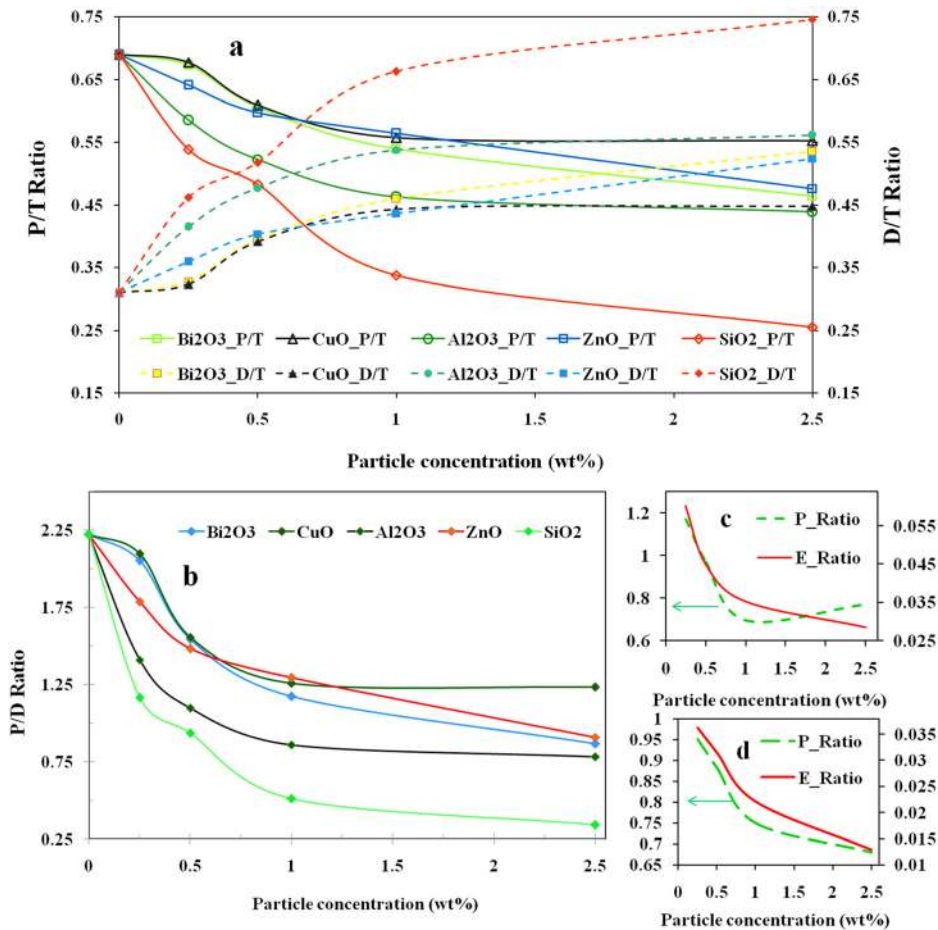


FIG. 5. (a) Variation of polar and dispersive components of surface tension to total surface tension of various nanofluids at different particle concentrations. (b) Variation of polar to dispersive components of surface tension at different particle concentrations for different nanofluids. (c) and (d) Electrical conductivity ratio (E_Ratio) and polar component ratio (P_Ratio) of nanofluids to that of water for CuO and Al₂O₃ nanoparticles based nanofluids, respectively.

half contribution to the total surface tension. As the particle population increases in the base fluid, it enhances and adds up the London dispersion interactions, Keesom interactions and also the Debye interactions, and hence results in an augmentation of the total van der Waals interaction in the colloidal system. There will be multiple and many-body interactions possible between the different particles, and the total will be the net vector resultant of the combined interaction forces. As the particle loading in the given colloidal solution increases, the spacing between the dispersed phase decreases. This can affect the total van der Waals interaction as well as the polar interactions due to the permanent polarity created due to the formation of an Electrical Double Layer (EDL) around the particle. It may be due to this electrostatic interaction that the effective dispersive interaction saturates after a certain value of particle loading. The steric repulsion between the particles start to dominate, and this may act against the attractive van der Waals interaction.

The polar to dispersive ratio of the nanoparticulate suspension is illustrated in Fig. 5(b). Comparing the ratio between the dispersive and polar parts of the surface energy/tension for two phases allows for a prediction of the adhesion between these two phases. The closer the ratios match more interactions are possible between the phases and higher the adhesion is to be expected. This helps one to choose a proper wetting surface and also quantify the net adhesion when a complex fluid such as a nanofluid interacts with a solid. Moreover, information about the P/D ratio of a given colloidal

solution can assist in assessing the wettability on a surface of known P/D ratio. Depending on the properties of the particles, the colloidal solution exhibited different P/D ratios and most of the suspension systems such as CuO, ZnO, and Bi₂O₃ remained with a predominant polar component throughout the entire concentrations of the particle considered, whereas the other particles exhibited a predominating polar nature up to about 0.5 wt. % of particle concentration. It is interesting to note that just by the addition of a trace amount of particles such as 0.1% by weight, the P/D ratio came down to nearly 1.25 from that of about 2.25 for the base fluid, which means a reduction of $\sim 45\%$. The high potential for interaction between two phases also leads to a small interfacial energy/tension.

A deeper insight into the physics of the nanoscale mechanisms at the interface shows that the wettability of the particle is an important parameter affecting the surface tension of the colloidal suspensions.³⁰ The interfacial adsorption characteristics are largely influenced by the adsorption-desorption characteristics of the particle, and the energetics of adsorption-desorption is given by³¹

$$\Delta E_p = -\pi\gamma R^2(1 + \cos\theta)^2. \quad (6)$$

Hence, it can be observed that the wettability of the particle at the nano-interface (θ), the size of the particle (R) (for non-spherical particles such as Bi₂O₃, the geometrically effective equivalent diameter has been considered or essentially the

diameter of gyration of the nanostructure) affects the energetics of adsorption-desorption characteristics and hence influences the surface tension of the colloidal solution. It may be noted that for the nanoscale particles, these energetics of adsorption-desorption are susceptible to thermal fluctuations since the order of magnitude of energetic is of the order of $\sim k_B T$ and may be subjected to thermal escape from the interface. These factors together with the Brownian dynamics of the particles determines the effective surface tension in such colloidal solutions and hence the constituent elements of total surface tension. This will be reflected in the wetting characteristics of the nanocolloidal solutions²⁷ on different substrates. Hence, these interactions are captured by our protocol for the measurement of the components of the interfacial tension through the macroscopic contact angle that is being used as an input parameter in the modified Owen Wendt protocol.

Figures 5(c) and 5(d) illustrate the polar component ratio and the electrical conductivity ratio (as outlined in the case of aqueous surfactant solutions) for the CuO and Al₂O₃ nanocolloidal suspensions. There are three major interacting modes with independent yet simultaneous existence (as outlined by Dhar *et al.*³²) found to be responsible for electrical transport in such colloidal systems. Electric double layer (EDL) formation at the nanoparticle–fluid interface-conjugated electrophoresis, nanoparticle polarization due to short-range field non-uniformity caused by the EDL with consequent particle motion due to inter-particle electrostatic interactions and coupled electro-thermal diffusion arising out of Brownian randomization in the presence of an electric field are described to be the three main mechanisms. Polarizability of the particle is an important characteristic property which affects the polar nature of the colloidal solution.¹⁰ The difference in magnitude of the polar component and its variation with respect to the concentration of the dispersed phase can be attributed to the difference in polarizability of different particles which are considered to be its characteristic property.³³ The polarizability of the particle is related to the pair potential as¹⁰

$$\mu_{11} = \frac{3\alpha_1^2 I_1}{4r_{11}^6}, \quad (7)$$

where α_1 is the polarizability, I_1 is the ionisation potential and r_{11} is the intermolecular distance, and the subscript 1 refers to a particular phase. The summation of all the pair potentials of all the volume elements can give an estimate of the dispersive component as

$$\gamma_1^d = \frac{-\pi N_1^2 \alpha_1^2 I_1}{8r_{11}^2}. \quad (8)$$

It can be observed that the polarizability, the ionisation potential and the packing fraction of the volume elements are important in contributing to the total dispersive energy. Also, the Hamaker constant is related to the polarizability as

$$A_1 = \frac{3}{4} N_1^2 \pi^2 \alpha_1^2 I_1. \quad (9)$$

However, as per the CDM principle, if N number of these atoms are brought together and allowed to interact, the

dipole-dipole interactions will influence the electric properties of the cluster, as a whole. In general, the total polarizability of the cluster cannot be expected to be equal to $N\alpha$, but will instead be modified because the atoms are subject to each other's induced electric field.²³ Also, the polarizability of the particle will influence the counter ion distribution, and hence the total polar interactions of the suspension and the modified Poissule equation has to be used³⁴ to understand the effective polar interactions in such complex suspensions. The similarity in the behavior of the electrical conductivity ratio with the particle concentration and the ratio of the polar component of the colloid to that of water as illustrated in Figs. 5(c) and 5(d) prove the present proposed hypothesis about the polar interactions in such colloidal suspensions.

A closer inspection of the influence of different particles in altering the polar nature of the base fluid can be observed from Fig. 6(a) illustrating the variation of the polar component of the colloidal solution to that of water. Bi₂O₃ shows an enhanced dominance of the polar component compared to that of other particles followed by CuO, ZnO, Al₂O₃ and the lowest by SiO₂. The observations depend upon the individual particle polarisability which ultimately is reflected in the form of a net polar component of surface tension. The normalized polar component ratio as illustrated in Fig. 6(a) indicates that the polar contribution to the total surface tension of the colloidal solution decreases with particle loading as the ratio is lower than 1 at all concentrations. Figure 6(b) illustrates the polar component ratio (designated as the P_Ratio which represents the ratio of the polar component of the colloidal suspension to that of the water) and the effective dielectric constant of the colloidal suspension (designated as DC) for the CuO nanocolloidal system. It can be observed that the mode of variation of both the quantities is similar. The dielectric constant value is an indication of the system resistance to polarizability and hence also indicates the electrical conductivity of the system, which is again indirectly related to the electrical conductivity and hence the polar nature of the fluid. Considering the nanoparticle to be a solid dielectric sphere with the potential within the sphere

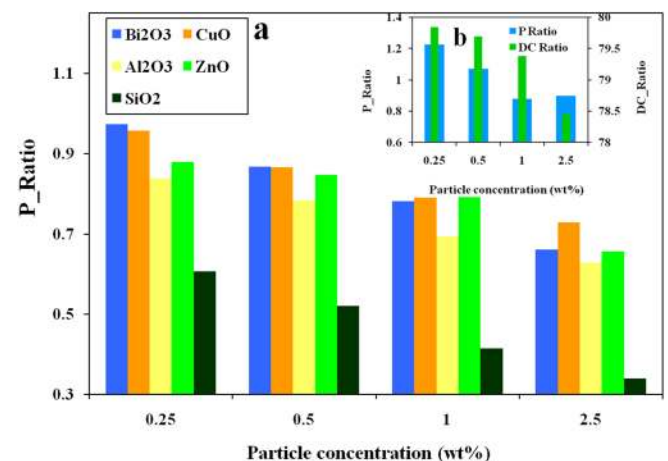


FIG. 6. (a) Variation of the ratio of the polar component of different nano-fluids to the polar component of water (P_Ratio) with particle concentration and (b) variation of the P_Ratio and the ratio of dielectric constant of nano-fluids to that of water (DC_Ratio) with particle concentration.

satisfying Laplace equation, the dipole moment “ p ” induced per nanoparticle in correspondence to the perturbed near field, as predicted by Clausius–Mosotti theorem, is expressed as³²

$$p = 4\pi\epsilon_0 k_f \left(\frac{d}{2}\right)^3 \frac{k_{np} - k_f}{k_{np} + 2k_f} E, \quad (10)$$

where k_f is the relative permittivity of the fluid and k_{np} represents the relative permittivity of the nanoparticle. From the above relation, we can understand the intertwined relation between the dielectric properties of the medium and the conductivity properties. The interactions of the external electric field with the randomly distributed, partially charged polar fluid molecules within the diffuse Guoy–Chapman layer promote the formation of non-uniformity in the effective field in the immediate circumferential neighbourhood of the nanoparticle. The existence of a spatio-temporally variant non-uniform electric field in the near vicinity of the nanoparticle leads to induced polarization of the particle. The fluctuating nature of the short-range electric field is a dependent function of the characteristics of the Guoy–Chapman layer. Since the layer is diffused by nature due to the presence of randomized electrostatic and thermal interactions among the polar fluid molecules, the concentration of the dispersed nanoparticulate phase and the temperature of the nanocolloid are important governing parameters responsible for the degree of particle polarization. Although spatio-temporally perturbed due to the innate nature of the electric field around the peripheral neighborhood, the magnitude of the dipole moment induced on the nanoparticle can be assumed to remain constant, given the near-spherical geometry of the particles. Hence, there exists an intertwining relationship among the polar interactions of the colloidal suspension and the electrical properties of the same.

The physics of interaction of the combined particle and the surfactant is a very complex phenomenon and can drastically alter the interfacial phenomenon such as surface tension and wetting.¹ Recently, there were a few studies probing the physics of the effect of nano-dispersions on the surface tension behavior^{1,31} and the fate of the nano-dispersed phase at the interface.³⁰ A recent study by present authors¹ has concluded that the combined particle and surfactant system exhibited a surface tension different from that of the particle only case and the aqueous surfactant only case, and the combined effect is not additive of individual effects. The combined system displayed a surface tension lower than the surfactant, and the enhanced population of the surfactant molecule at the interface due to transport by surfactant capped nanoparticles¹ was outlined to be the main mechanism responsible for such an anomalous behavior. Due to the inherent attraction of surfactants to the interface and the nanoparticles being in dynamic random motion due to thermal fluctuations will facilitate populating the interface with more nanoparticles due to the transport of surfactant capped nanoparticles. The surface tension decreases initially with the particle concentration, and then an almost negligible change is observed with respect to the particle concentration at a given surfactant concentration due to the steric hindrance preventing the further adsorption onto the interface.

In order to track the contribution of combined particle and surfactant molecules or a surfactant capped nano-dispersion system in modulating the polar and dispersive interactions of the colloidal solution, the study has been extended to dispersions where the surfactant molecules are also infused during the preparation and homogenisation of nano-dispersions. The study conducted at different concentrations of surfactants and particles will help to elucidate the influence and contributions of individual components, and the net total effect in amending the nature of surface energy. As the surface tension is a surface phenomenon, the interface plays an important role and the presence of strong surface active agents bonded to the nanoparticles can drastically alter the wetting dynamics. Nanocolloidal solutions containing only particles showed an increment in the contact angle on silicon and glass substrates, whereas it decreases initially and then increases with particle concentration on aluminium and copper substrates.²⁷ However, as expected, the contact angle of surfactants decreases with the surfactant concentration as expected.²⁷ With the increase in the particle concentration, the static contact angle decreases initially and then exhibited almost a negligible change with particle concentration for the combined surfactant and particle case. However, with the increase in the surfactant concentration, the contact angle decreases at a given particle concentration. We observed that the surfactant effect dominated in the case of combined surfactant and particle with respect to the wetting phenomenon and the combined colloidal system exhibited a similar wetting behaviour irrespective of the surface which is in accordance with the earlier reported literature.²⁷

The variation of normalised surface tension components of MWCNTs and SDS colloidal solution with the particle concentration at different surfactant concentrations (in terms of CMC) is illustrated in Fig. 7(a). There is a slight dip in the value of the D/T ratio at a very small concentration of particles and thereafter the ratio keeps increasing with the particle concentration for a given surfactant concentration. Similarly, there is an initial hump in the P/T ratio and thereafter it steadily decreases with CNT concentration up to the maximum concentration of 0.25 wt. % considered in the present study. This can be attributed to the high surface charge density of the CNT particles due to which the EDL will be strong and the potential will be much higher compared to other particles. Due to the anomalous pull created by the CNT particles, the polar interactions in the fluid will be so strong that it may overshadow and will be a dominant source of total surface tension. Moreover, the packing of surfactant molecules over the surface of carbon nanotubes will enhance the EDL and result in the induction of more polar nature. But, with the increase in the CNT concentration, the dispersive interaction between the long carbon will start to dominate and increase with the particle concentration at a given surfactant concentration. Also interestingly, the initial dip is more prominent at lower surfactant concentrations, as towards higher surfactant concentrations, the hydrocarbon chain interaction resulting in the van der Waals interaction, steric interactions due to hydrocarbon chains, etc., will also come into play. So, the net effect will be the summation of all the individual effects. The polar to dispersive ratio also

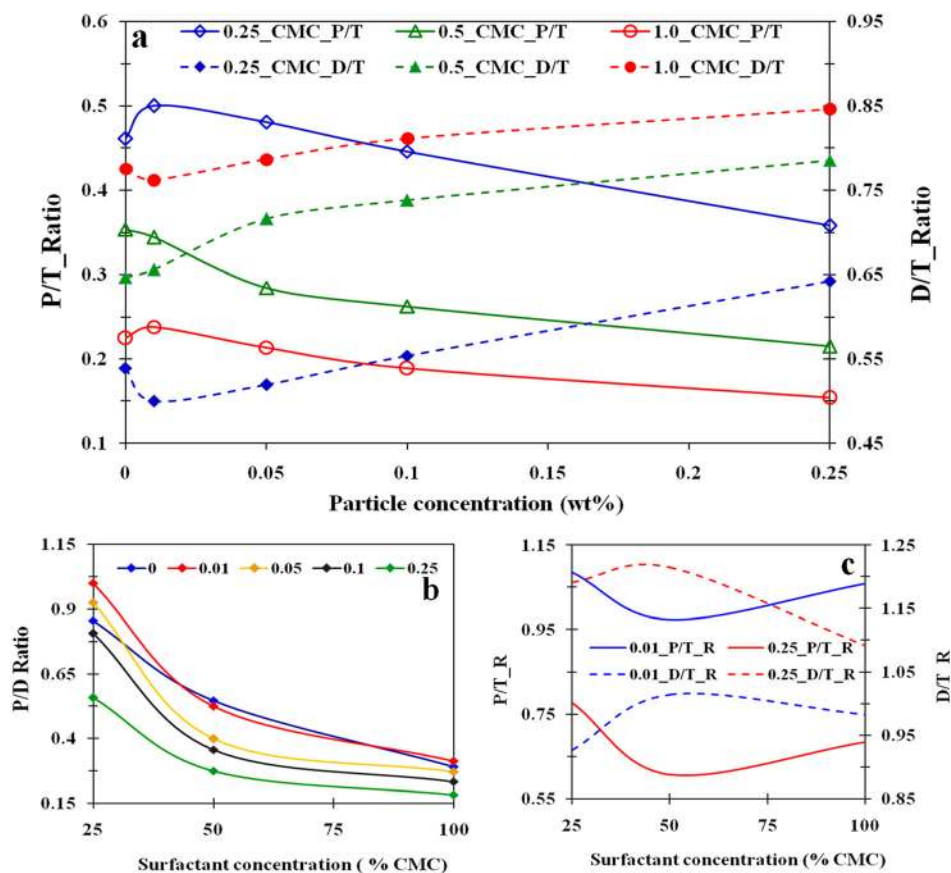


FIG. 7. (a) Ratio of polar to total surface tension and dispersive to total surface tension values for MWCNTs with SDS surfactant at three surfactant concentrations (in terms of CMC) at various particle concentrations (b) variation of the ratio of polar to dispersive component of surface tension with surfactant concentration at various particle concentrations for the above particle and surfactant combination (c) normalized polar to total value of surface tension (normalized with that of the aqueous surfactant solution) with surfactant concentration for a given particle concentration.

showcased an exponential decay with the particle concentration as illustrated in Fig. 7(b). It is clear from Fig. 7(c) that the physics of interaction in the case of surfactant capped nanosuspensions is altogether different from the suspensions of surfactant alone or particle alone cases as the surfactant concentration plays an important role in determining the polar and dispersive interactions of the combined colloidal system. With the increase in surfactant concentration at a given CNT concentration, the D/T ratio increases and then decreases, whereas the P/T ratio decreases and then increases. As discussed earlier, this stems from the interplay of electrostatic interactions and other interactions present in such complex systems.

Figure 8(a) illustrates the polar to total surface tension ratio (P/T ratio) and the ratio of the dispersive component to the total surface tension of the fluid (D/T ratio) for the combined SDS and CuO nanofluids with the CuO concentration at three surfactant concentrations. Even though the general trend of decreasing and then attaining a plateau shape for the P/T ratio is conserved as in the case of only nanoparticle suspensions and aqueous surfactant solutions, the combined surfactant and nanoparticle case reached saturation early at a lower value of particle concentration itself. This trend is true in the case of all the surfactant concentrations. The D/T ratio is following just a mirror inversion of the other ratio. Also, it can be observed that at a given particle concentration the P/T ratio decreases with the surfactant concentration, whereas the D/T ratio increases with the surfactant concentration for all concentrations of particles. Moreover, it can be observed that there is a sharp decrement in the value of the P/T ratio

with a trace amount of particle addition at 0.1 wt. % at 0.25 CMC, whereas at CMC, the decrement is much shallow. The ratio of polar to dispersive component also decreases and then saturates with an increase in particle concentration as illustrated in Fig. 8(b) and the decrease is sharp at lower particle concentrations of the surfactant and eventually decreases with an increment in the surfactant concentration. Zero particle concentration of the P/D ratio corresponds to that of the aqueous surfactant solution at a given particular surfactant concentration. As the surfactant concentration increases, the EDL become strong and the electrostatic interactions dominate and hence there is only a minor dip in the value of P/D ratio.

The ratio of the P/D ratio of SDS and CuO based nanofluid to that of DTAB (Dodecyltrimethylammonium bromide) and CuO based nanocolloid is illustrated in Fig. 8(c). This represents the relative strength of the two surfactants considered in the present study for the same CuO nanoparticles. There is an observable dip in the value of ratio of the P/D ratio with concentration initially and then steadily it remains almost constant at 0.25 CMC and 0.5 CMC, whereas at a higher surfactant concentration than the CMC instead of an initial dip an increment is being observed. This again depends on the relative strength of thickening of the EDL and hence on the polar interactions in the presence of two surfactants. It can be observed that the SDS is more effective at higher surfactant concentrations in modulating the polar component of surface tension. At almost all instants of concentration, the ratio remains less than 1 indicating the predominant role of the polar component in the case of DTAB and CuO based nanofluids. The ratio gives a comparative picture of how for

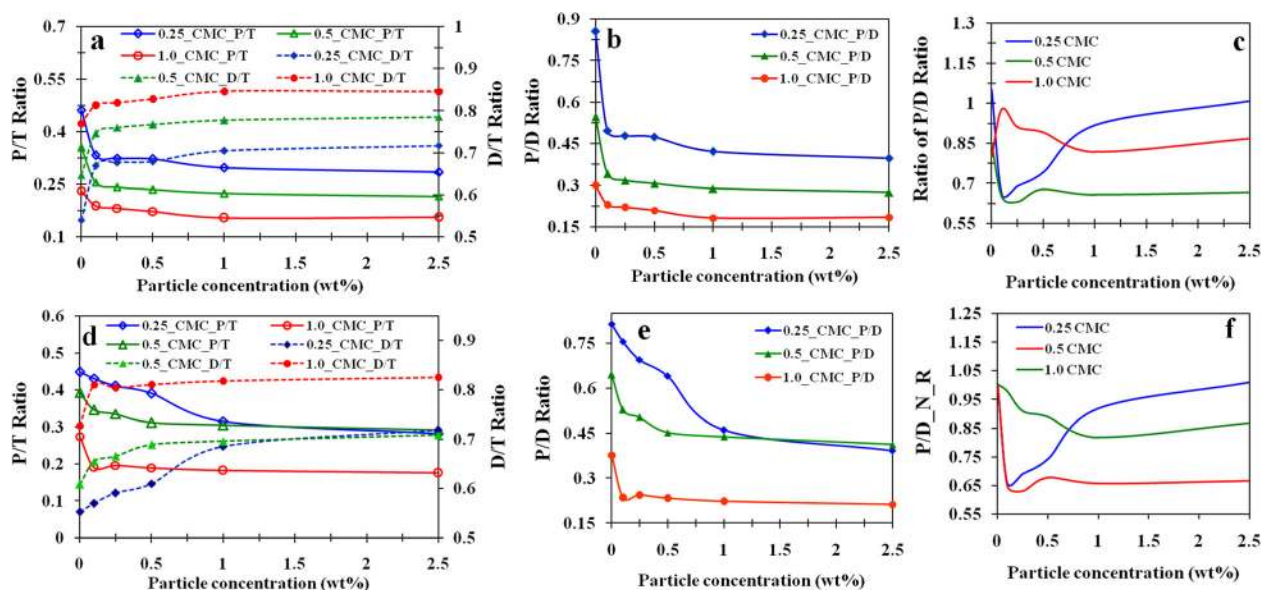


FIG. 8. For CuO and SDS nanocolloidal suspension, (a) illustrates the variation of the ratio of polar and dispersive components of surface tension to the total surface tension of a combined colloidal system (represented as P/T ratio and D/T ratio, respectively) with particle concentration (b) the variation of ratio of polar to dispersive components of surface tension (P/D ratio) with particle concentration at three surfactant concentrations of 0.25, 0.5, and 1.0 times the CMC concentration (c) ratio of the P/D ratio for a CuO and SDS based nanocolloid to that of a CuO and DTAB nanocolloid at different particle concentrations at three surfactant concentrations (d) variation of the P/T ratio and the D/T ratio with an increase in particle concentration for a CuO and DTAB based nanocolloid (e) variation of the ratio of polar to dispersive components of surface tension (P/D ratio) with particle concentration at three surfactant concentrations for CuO and DTAB based nanocolloids (f) the variation of the ratio of normalized (normalized with that of the value of a surfactant at a given surfactant concentration) P/D ratio of a CuO and SDS based nanocolloid with that of the normalized P/D ratio of a CuO and DTAB based nanocolloid.

the same nanoparticles but with two different surfactants one is able to modulate the polar and dispersive components. It can be concluded that for a given particle, SDS tends to make the solution more dispersive, whereas DTAB tries to make the solution relatively more polar in nature. The nature of the P/D ratio variation in the case of DTAB and CuO based nanocolloid is also similar to that of the SDS and CuO based nanocolloid as illustrated in Fig. 8(e). The observations are similar to that observed in the case of CuO and SDS based nanocolloid. The normalized P/D ratio (ratio of the P/D value of colloid to the P/D value of aqueous surfactant) represents the amount of increment or decrement the particle has brought out in the combined colloidal system compared to the value of the P/D ratio in the case of an aqueous surfactant solution. Figure 8(f) illustrates the ratio of the normalized P/D ratio of CuO and SDS based nanocolloid to that of CuO and DTAB surfactant. The normalized curves less than unity indicate that CuO is more active in modulating the polar and dispersive interactions in the combined colloidal system of CuO and DTAB than CuO and SDS. However, the amount of modulations varies with respect to the surfactant concentration in the combined colloidal system.

Figures 9(a)–9(f) illustrates the same analysis extended to the Bi_2O_3 nanoparticles with SDS and CTAB surfactants. The nature of variation of polar to total surface tension and the dispersive component to total surface tension is similar as observed in earlier case for both the surfactant combinations. However, the magnitude of modulation is different in each case. The nature of variation of the polar to dispersive component of surface tension is also the same at all surfactant concentrations even though the morphology of the nanoparticle is entirely different from that of CuO nanoparticles.

The ratio of the P/D ratio in both the colloidal systems value greater than unity indicates the predominating polar effect in a SDS based Bi_2O_3 nanofluid compared to that with CTAB at all concentrations of the surfactant. Figure 9(f) illustrates the ratio of the normalized P/D ratio of a Bi_2O_3 and SDS based nanocolloid to that of a Bi_2O_3 and CTAB surfactant. The normalized curves attain values less than unity at higher surfactant concentrations which indicate that Bi_2O_3 is more active in modulating the polar and dispersive interactions in the combined colloidal system of Bi_2O_3 and CTAB than Bi_2O_3 and SDS above 0.25 CMC surfactant concentrations. However, the amount of modulations varies with respect to the surfactant concentration in the combined colloidal system. A comparative analysis of the polar and dispersive interactions in MWCNTs and SDS based colloidal suspension and CuO and SDS based colloidal suspension is presented in the [supplementary material](#). In précis, the present work is able to portray that the observations can be merged into a form of quasi-universal behavior in the trends of polar and dispersive components in spite of non-universal character in the wetting behavior of the nanocolloids, aqueous surfactant and surfactant integrated nanocolloids.

V. CONCLUSIONS

A comprehensive experimental study has been employed to extract the polar and dispersive components of surface tension in nanocolloids using a reverse Owen Wendt scheme. The surface tension of nanocolloids obtained using a pendant tensiometric method, earlier reported literature values of surface tension in nanosuspensions, experimentally measured contact angle data on different substrates, and

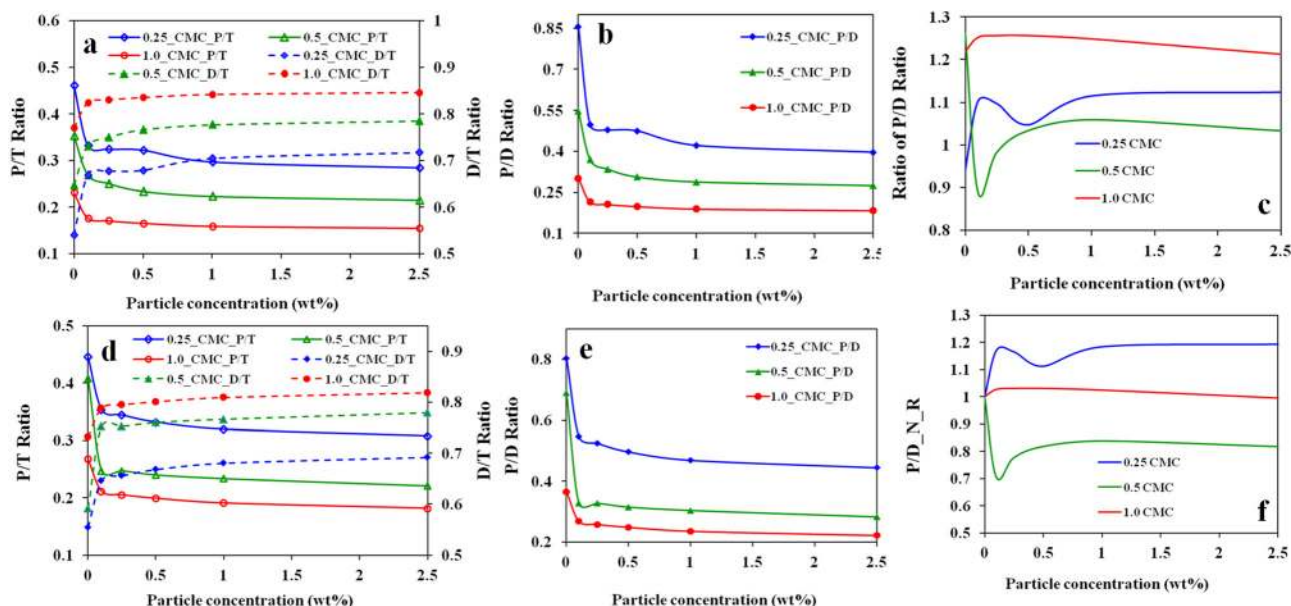


FIG. 9. For a Bi_2O_3 and SDS based nanocolloidal suspension, (a) illustrates the variation of the ratio of polar and dispersive components of surface tension to the total surface tension of a combined colloidal system (represented as P/T ratio and D/T ratio, respectively) with particle concentration (b) the variation of the ratio of polar to dispersive components of surface tension (P/D ratio) with particle concentration at three surfactant concentrations of 0.25, 0.5, and 1.0 times the CMC concentration (c) ratio of the P/D ratio for a Bi_2O_3 and SDS based nanocolloid to that of a Bi_2O_3 and CTAB nanocolloid at different particle concentrations at three surfactant concentrations (d) variation of the P/T ratio and the D/T ratio with particle concentration for a Bi_2O_3 and CTAB based nanocolloid (e) variation of the ratio of polar to dispersive components of surface tension (P/D ratio) with particle concentration at three surfactant concentrations for Bi_2O_3 and CTAB based nanocolloids (f) the variation of the ratio of normalized (normalized with that of the value of surfactant at a given surfactant concentration) P/D ratio of a Bi_2O_3 and SDS based nanocolloid with that of the Bi_2O_3 and CTAB based nanocolloid.

experimentally determined surface energies of the substrate using the Owens Wendt method are used as input parameters in determining and segregating the dispersive and polar interactions in nanofluids. The effect of surfactants in aqueous solutions, the presence of dispersed nanosized particles and the combined effect of surfactants and nanoparticles in altering the contributive component of surface tension have been studied, and the effect of concentration and the ratio of mixing particles and surfactants have also been extracted. An extensive theoretical framework has been proposed in the light of DLVO and non-DLVO interactions in the colloids to enhance the understanding of governing physics behind the interactions. The present study reveals findings that may have strong implications towards expanding the understanding of interfacial phenomena in complex fluids and its applicability in different fields of engineering.

SUPPLEMENTARY MATERIAL

See [supplementary material](#) for the algorithm of inverse protocol for the classical Owen Wendt Method and a comparative analysis of polar and dispersive interactions in MWCNTs and SDS based nanocolloids with those in CuO and SDS based nanocolloids.

ACKNOWLEDGMENTS

A.R.H. would like to thank the Ministry of Human Resources, Government of India for the doctoral scholarship. P.D. would like to acknowledge the funding by IIT Ropar (Grant Sanction No. IITRPR/Research/193 and IITRPR/Interdisciplinary/CDT).

- ¹A. R. Harikrishnan, P. Dhar, P. K. Agnihotri, S. Gedupudi, and S. K. Das, "Effects of interplay of nanoparticles, surfactants and base fluid on the surface tension of nanocolloids," *Eur. Phys. J. E* **40**(5), 53 (2017).
- ²S. S. Khaleduzzaman, I. M. Mahbulul, I. M. Shahrul, and R. Saidur, "Effect of particle concentration, temperature and surfactant on surface tension of nanofluids," *Int. Commun. Heat Mass Transfer* **49**, 110–114 (2013).
- ³R. G. Chaudhuri and S. Paria, "The wettability of PTFE and glass surfaces by nanofluids," *J. Colloid Interface Sci.* **434**, 141–151 (2014).
- ⁴L. Espín and S. Kumar, "Forced spreading of films and droplets of colloidal suspensions," *J. Fluid Mech.* **742**, 495 (2014).
- ⁵T. A. Nguyen and A. V. Nguyen, "Increased evaporation kinetics of sessile droplets by using nanoparticles," *Langmuir* **28**, 16725–16728 (2012).
- ⁶A. Crivoi, X. Zhong, and F. Duan, "Crossover from the coffee-ring effect to the uniform deposit caused by irreversible cluster-cluster aggregation," *Phys. Rev. E* **92**, 032302 (2015).
- ⁷F. Carle and D. Brutin, "How surface functional groups influence fracturation in nanofluid droplet dry-outs," *Langmuir* **29**, 9962–9966 (2013).
- ⁸L. Bansal, A. Miglani, and S. Basu, "Morphological transitions and buckling characteristics in a nanoparticle-laden sessile droplet resting on a heated hydrophobic substrate," *Phys. Rev. E* **93**, 042605 (2016).
- ⁹L. A. Girifalco and R. J. Good, "A theory for the estimation of surface and interfacial energies. I. Derivation and application to interfacial tension," *J. Phys. Chem.* **61**, 904–909 (1957).
- ¹⁰F. M. Fowkes, "Attractive forces at interfaces," *Ind. Eng. Chem.* **56**, 40–52 (1964).
- ¹¹F. M. Fowkes, "Calculation of work of adhesion by pair potential summation," *J. Colloid Interface Sci.* **28**, 493–505 (1968).
- ¹²D. K. Owens and R. C. Wendt, "Estimation of the surface free energy of polymers," *J. Appl. Polym. Sci.* **13**, 1741–1747 (1969).
- ¹³S. Wu, "Polar and nonpolar interactions in adhesion," *J. Adhes.* **5**, 39–55 (1973).
- ¹⁴C. J. Van Oss, R. J. Good, and M. K. Chaudhury, "The role of van der Waals forces and hydrogen bonds in 'hydrophobic interactions' between biopolymers and low energy surfaces," *J. Colloid Interface Sci.* **111**, 378–390 (1986).
- ¹⁵T. Nguyen and W. E. Johns, "Polar and dispersion force contributions to the total surface free energy of wood," *Wood Sci. Technol.* **12**, 63–74 (1978).

- ¹⁶F. Carle, S. Semenov, M. Medale, and D. Brutin, "Contribution of convective transport to evaporation of sessile droplets: Empirical model." *International Journal of Thermal Sciences* **101**, 35–47 (2016).
- ¹⁷Y. C. Hong, D. H. Shin, S. C. Cho, and H. S. Uhm, "Surface transformation of carbon nanotube powder into super-hydrophobic and measurement of wettability," *Chem. Phys. Lett.* **427**, 390–393 (2006).
- ¹⁸S. Kumar and V. K. Aswal, "Tuning of nanoparticle-surfactant interactions in aqueous system," *J. Phys.: Condens. Matter* **23**, 035101 (2010).
- ¹⁹C. Pfeiffer, C. Rehbock, D. Hühn, C. Carrillo-Carrion, D. J. de Aberasturi, V. Merk, S. Barcikowski, and W. J. Parak, "Interaction of colloidal nanoparticles with their local environment: The (ionic) nanoenvironment around nanoparticles is different from bulk and determines the physico-chemical properties of the nanoparticles," *J. R. Soc., Interface* **11**, 20130931 (2014).
- ²⁰M. Zenkiewicz, "New method of analysis of the surface free energy of polymeric materials calculated with Owens-Wendt and Neumann methods," *Polimery* **51**, 584–587 (2006).
- ²¹B. V. Derjaguin, "Theory of the stability of strongly charged lyophobic sols and the adhesion of strongly charged particles in solutions of electrolytes," *Acta Physicochim. USSR* **14**, 633–662 (1941).
- ²²E. J. W. Verwey and J. T. G. Overbeek, *Theory of the Stability of Lyophobic Colloids* (Elsevier, New York, 1948).
- ²³B. W. Kwaadgras, M. Verdult, M. Dijkstra, and R. van Roij, "Polarizability and alignment of dielectric nanoparticles in an external electric field: Bowls, dumbbells, and cuboids," *J. Chem. Phys.* **135**, 134105 (2011).
- ²⁴H. C. Hamaker, "The London—van der Waals attraction between spherical particles," *Physica* **4**, 1058–1072 (1937).
- ²⁵C. J. Van Oss, R. J. Good, and M. K. Chaudhury, "Additive and nonadditive surface tension components and the interpretation of contact angles," *Langmuir* **4**, 884–891 (1988).
- ²⁶J. Eastoe and J. S. Dalton, "Dynamic surface tension and adsorption mechanisms of surfactants at the air–water interface," *Adv. Colloid Interface Sci.* **85**, 103–144 (2000).
- ²⁷A. R. Harikrishnan, P. Dhar, P. K. Agnihotri, S. Gedupudi, and S. K. Das, "Wettability of complex fluids and surfactant capped nanoparticle-induced quasi-universal wetting behaviour," *J. Phys. Chem. B* **121**, 6081–6095 (2017).
- ²⁸A. J. B. Milne, J. A. W. Elliott, P. Zabeti, J. Zhou, and A. Amirfazli, "Model and experimental studies for contact angles of surfactant solutions on rough and smooth hydrophobic surfaces," *Phys. Chem. Chem. Phys.* **13**(36), 16208–16219 (2011).
- ²⁹K. L. Herrington, E. W. Kaler, D. D. Miller, J. A. Zasadzinski, and S. Chiruvolu, "Phase-behavior of aqueous mixtures of dodecyltrimethylammonium bromide (DTAB) and sodium dodecyl-sulfate (SDS)," *J. Phys. Chem.* **97**, 13792–13802 (1993).
- ³⁰V. Garbin, I. Jenkins, T. Sinno, J. C. Crocker, and K. J. Stebe, "Interactions and stress relaxation in monolayers of soft nanoparticles at fluid-fluid interfaces," *Phys. Rev. Lett.* **114**, 108301 (2015).
- ³¹C. Zeng, H. Bissig, and A. D. Dinsmore, "Particles on droplets: From fundamental physics to novel materials," *Solid State Commun.* **139**, 547–556 (2006).
- ³²P. Dhar, A. Pattamatta, and S. K. Das, "Trimodal charge transport in polar liquid-based dilute nanoparticulate colloidal dispersions," *J. Nanopart. Res.* **16**, 2644 (2014).
- ³³E. Sahagún and J. J. Sáenz, "Dielectric nanoparticles: Polarizability reveals identity," *Nat. Mater.* **11**, 748–749 (2012).
- ³⁴A. Bakhshandeh, A. P. Dos Santos, and Y. Levin, "Weak and strong coupling theories for polarizable colloids and nanoparticles," *Phys. Rev. Lett.* **107**, 107801 (2011).